

# Dual-Energy Head Cone-Beam CT Using a Dual-Layer Flat-Panel Detector: Physics-Based Material Decomposition

Zhilei Wang<sup>a</sup>, Hao Zhou<sup>a</sup>, Shan Gu<sup>a</sup>, and Hwei Gao<sup>\*a</sup>

<sup>a</sup>Department of Engineering Physics, Tsinghua University, Beijing 100084, China

## ABSTRACT

Flat panel detector (FPD) based cone-beam computed tomography (CT) has made tremendous progress these days, with many new medical and industrial applications keeping emerging from diagnostic imaging and image guidance for radiotherapy and interventional surgery. However, current cone-beam CT (CBCT) is still suboptimal for head scan whose requirement for image quality is extremely strict. Recently, the dual-layer flat panel detector technology is under development and is promising to further advance CBCT from qualitative anatomic imaging to quantitative dual-energy CT. Its potential of enabling head CBCT applications has yet been investigated. The relatively moderate energy separation from the dual-layer FPD and the overall low signal level especially for the bottom layer detector, raise significant challenges in performing high quality dual-energy material decomposition. In this work, we propose a physics based material decomposition algorithm that attempts to fully use the detected X-ray signals and prior-knowledge behind head CBCT using dual-layer FPD. Specifically, projection data from the two layers of detector are first adaptively combined to generate conventional CT images with reduced noise. A physics model based dual-layer multi-material spectral correction (dMMSC) is then developed to make the combined image reconstruction beam-hardening free. After a regular projection-domain material decomposition (MD) being conducted, the corresponding beam-hardening free projections from the dMMSC will be taken as a guidance to further enhance the dual-layer MD performance, leading to significantly improved robustness of MD and suppressed low-signal artifact in our preliminary results.

**Keywords:** head cone-beam CT, material decomposition, dual energy imaging, dual-layer flat panel detector

## 1. INTRODUCTION

FPD-based CBCT has many advantages, such as low cost, high spatial resolution, and 3D imaging in single rotation that greatly improves the utilization of x-ray photons and reduce the radiation dose to patients. However, the overall image quality of CBCT can be easily compromised by beam hardening, scatter, and cone-beam artifacts,<sup>1</sup> impeding its further application in diagnostic imaging such as head scan which has strict requirements on the imaging performance.<sup>2</sup> The emergence of dual-layer flat-panel detector technology can enable dual-energy imaging without changing the conventional scanning protocol, providing extra means of improving CBCT image quality, with potentially material-specific information<sup>3,4</sup> However, besides X-ray scattering that is beyond the scope of this study, dual-layer flat panel detector based dual-energy CBCT has its own challenges due to its relatively moderate energy separation and the overall low signal level especially for the bottom layer detector. In this work, we attempt to explore the feasibility of having dual-energy head CBCT using a dual-layer FPD, and to develop a physics model guided material decomposition that fully uses the detected X-ray signals and the physics knowledge behind head CT imaging.

## 2. METHOD

### 2.1 Data acquisition from a dual-layer flat panel detector prototype

With a dual-layer FPD, dual-energy data can be acquired simultaneously. As illustrated in Fig. 1, a higher energy spectrum is obtained from the bottom layer which is essentially filtered by the top layer detector. Mathematically, low- and high-energy projections can be expressed as

---

\* Author to whom correspondence should be addressed. Email address: hwgao@tsinghua.edu.cn

$$\begin{aligned}
P_L &= -\ln \left( \frac{\int S(E) e^{-\int \mu(E) dl} \eta_T(E) dE}{\int S(E) \eta_T(E) dE} \right) \\
P_H &= -\ln \left( \frac{\int S(E) e^{-\sum \mu_i(E) D_i} e^{-\int \mu(E) dl} \eta_B(E) dE}{\int S(E) e^{-\sum \mu_i(E) D_i} \eta_B(E) dE} \right),
\end{aligned} \tag{1}$$

where,  $S(E)$  denotes the incident spectrum of source;  $\eta_T(E) \propto (1 - e^{-\mu_T(E) D_T}) E$  and  $\eta_B(E) \propto (1 - e^{-\mu_B(E) D_B}) E$  denote the detector responses of top layer and bottom layer, respectively;  $e^{-\sum \mu_i(E) D_i}$  denotes the attenuation of top-layer material and possible inter-layer filter;  $S(E) \cdot \eta_T(E)$  and  $S(E) e^{-\sum \mu_i(E) D_i} \cdot \eta_B(E)$  therefore indicate the overall detective spectra of low- and high-energy scan, respectively.

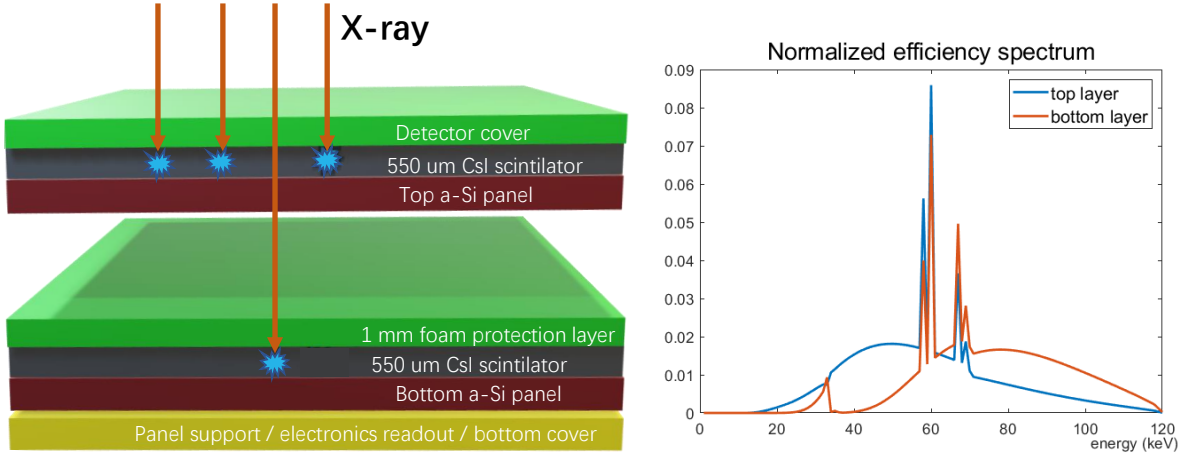


Figure 1. Left: The detailed structure of a prototype dual-layer FPD used in our study. Right: the normalized effective spectrum for top and bottom layer.

## 2.2 Reconstruction from combined dual-layer projections

On a dual-layer flat panel detector, the top layer is more likely to absorb low-energy x-ray photons, while relatively more high-energy x-ray photons are absorbed in the bottom layer. Naturally, by weighting two layers of projection data properly, noise reduction in the corresponding reconstruction will be achieved as more signals (x-ray photons) will be utilized. An optimal weight factor  $\omega$  can be determined by minimizing the noise on reconstructed images from combined dual-layer projections as below.

$$P_t = \omega P_L + (1 - \omega) P_H \tag{2}$$

## 2.3 Physics model-guided material decomposition

First, conventional head CT images with decreased noise are reconstructed from adaptively combined dual-layer projection data, followed by a dual-layer multi-material spectral correction (dMMSC) to generate beam hardening free images.<sup>5</sup> After a regular projection-domain material decomposition (MD) using dual-layer detector data that is usually quite sensitive to low-signal x-ray photon and energy separation, the dMMSC corrected projections are used as a physics-model based guidance to further enhance the dual-layer MD performance.

### 2.3.1 First-pass projection-domain material decomposition

For the dual-layer FPD, since the acquired low- and high-energy projections ( $P_L$ ,  $P_H$ ) are quite consistent both spatially and temporarily, it is better to perform a material decomposition in the projection domain so that beam hardening can be better eliminated. For a head scan using a dual-layer FPD, water and bone can be chosen as the basis materials. In this study, we employed a five-order polynomial fitting<sup>6</sup> to generate the basis

material projections. After image reconstruction from the basis material projections, two basis material CT images will be created. By weighting the two basis material images using their attenuation coefficients at a specific energy, a virtual monoenergetic (VM) image at that energy can be generated. Theoretically, the virtual monoenergetic images should be free from beam hardening artifacts. However, due to the sensitivity of MD to noise and energy separation, streaks can be easily observed in the VM images which significantly degrade the dual-energy performance from the dual-layer FPD.

### 2.3.2 Dual-layer multi-material spectral correction

As we know, due to the significant bony structures in human head, a water correction is not enough to remove beam hardening artifact in head CT images. In the literature, multi-material spectral correction has been developed as a poster-reconstruction method for conventional CT scan to estimate and correct for bone's beam hardening impact. In this work, we extend this kind of method to dual-layer projection data, which consists of the following steps. First, an initial reconstruction after water correction is conducted to estimate the distribution of bony structures that can be easily segmented out from soft tissues. Then, projection of bony structures  $P_b$  can be computed using forward projection. With the help of the bone projection, a multi-material spectra-corrected projection that is beam-hardening free can be computed as

$$P_{dMMSC} = P_t + f(P_t, P_b), \quad (3)$$

where,  $f(P_t, P_b)$  represents the bone-induced beam-hardening error and can be modeled and calculated in advance by simulations or measurements.

### 2.3.3 material decomposition enhancement using dMMSC

In order to improve the dual-energy performance from the dual-layer FPD, beam hardening free projections after dMMSC is adopted as a guidance to minimize the material decomposition errors and generate a high-quality head image. An optimal hybrid VM projections can be generated using an adaptive fusion of projection with dMMSC and VM projection at an efficient energy as

$$\tilde{P}_{VM}^{eff} = \lambda P_{VM}^{eff} + (1 - \lambda) P_{dMMSC}, \quad (4)$$

where,  $P_{dMMSC}$  and  $P_{VM}^{eff}$  denote the spectra-corrected projection and VM projection, respectively. Basis material projections can also be re-fined by using the hybrid VM projection at optimal keV and a VM projection generated at higher keV ( $P_{VM}^{high}$ ).

## 3. RESULTS

### 3.1 Experimental system set up

Our study is based on a benchtop CBCT system equipped with a prototype dual-layer FPD in our lab. The prototype dual layer FPD (Varex imaging, Salt Lake City, UT, USA) consists of two amorphous silicon (a-Si) panels with pixel size of  $150 \mu m$ , both deposited with a  $550 \mu m$ -thick CsI scintillator, with no additional intermediate filter placed in between [Fig. 2]. The source-to-axis distance was set to 750mm and the source-to-detector distance to 1184 mm. In our study, 720 projections over 360 degree were collected at 30 fps in a  $3 \times 3$  binning mode. The X-ray source (Varex Imaging G-242, Salt Lake City, UT, USA) at 120 kV, 64 mA and 5 ms of pulse width. In our current study, a narrowed X-ray collimation was implemented to get rid of X-ray scatter's impact which is another big challenge to CBCT spectral imaging but is under a separate investigation. In our study, a 120 kV X-ray source is used. The estimated effective spectrum for the top and bottom layer is shown in Fig. 1 and the average energy separation between low- and high-energy spectra can reach a level of 17 keV without object in the beam.

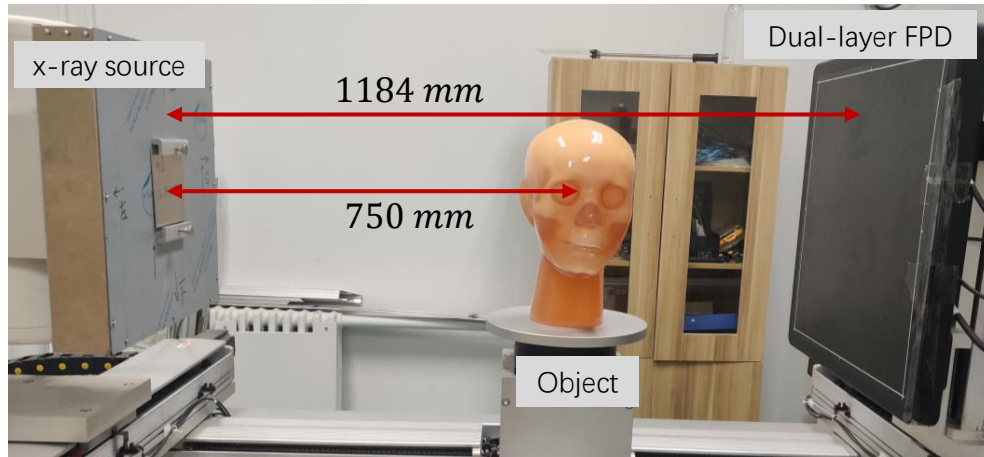


Figure 2. The benchtop CBCT system using DL FPD.

### 3.2 Combined reconstruction from dual-energy projections

By combining the dual layer projection data using different weighting factor, an optimal weighting factor can be determined empirically by measuring the standard deviations of selected ROIs. As shown in Fig. 3, the measurements of signal to noise ratio (SNR) on reconstructed images from top-layer, bottom-layer and combined data are shown beside the selected ROIs. Our preliminary results suggest that the standard deviation can be reduced by roughly 10% when compared with that of the top layer alone.

### 3.3 Physics model-guided material decomposition

The results of basis material decomposition of a head phantom are shown in Fig. 4. The VM images at 63 keV was generated and it is seen that most beam hardening artifacts caused by the bony objects are removed. However, in some locations strong streak artifacts occur badly in the CT images, which can be well suppressed by using our proposed approach. Firstly, we use the spectra-corrected projection at 63 keV as a guidance of VM projection at the same keV to generate an improved VM projection which is combined with generated VM image at 90 keV to refine the water and bone image. By using our physics based material decomposition, we can see that most streak artifacts can be removed in the basis material images and VM images.

## 4. CONCLUSION

In this work, we proposed a physics model guided material decomposition algorithm that is suitable for head CBCT using dual-layer FPD. Preliminary results using narrowed X-ray collimation on our benchtop dual-layer

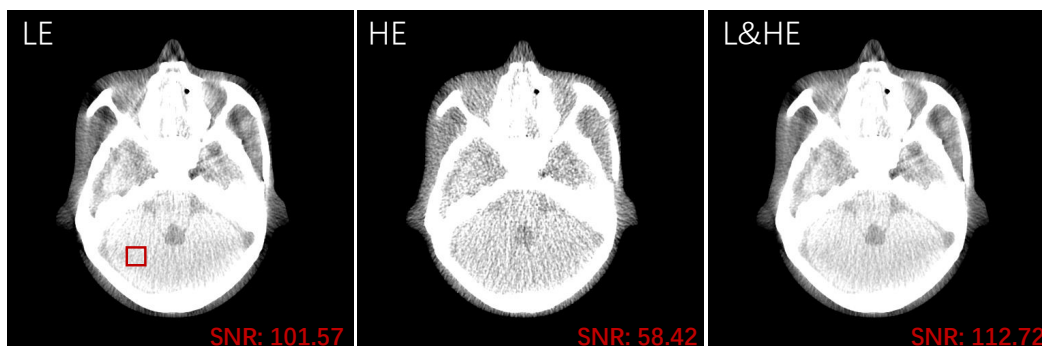


Figure 3. Reconstruction from low- and high-energy projections and our proposed weighted combination of the projections. Display window: [-100, 100] HU (Hounsfield Units).

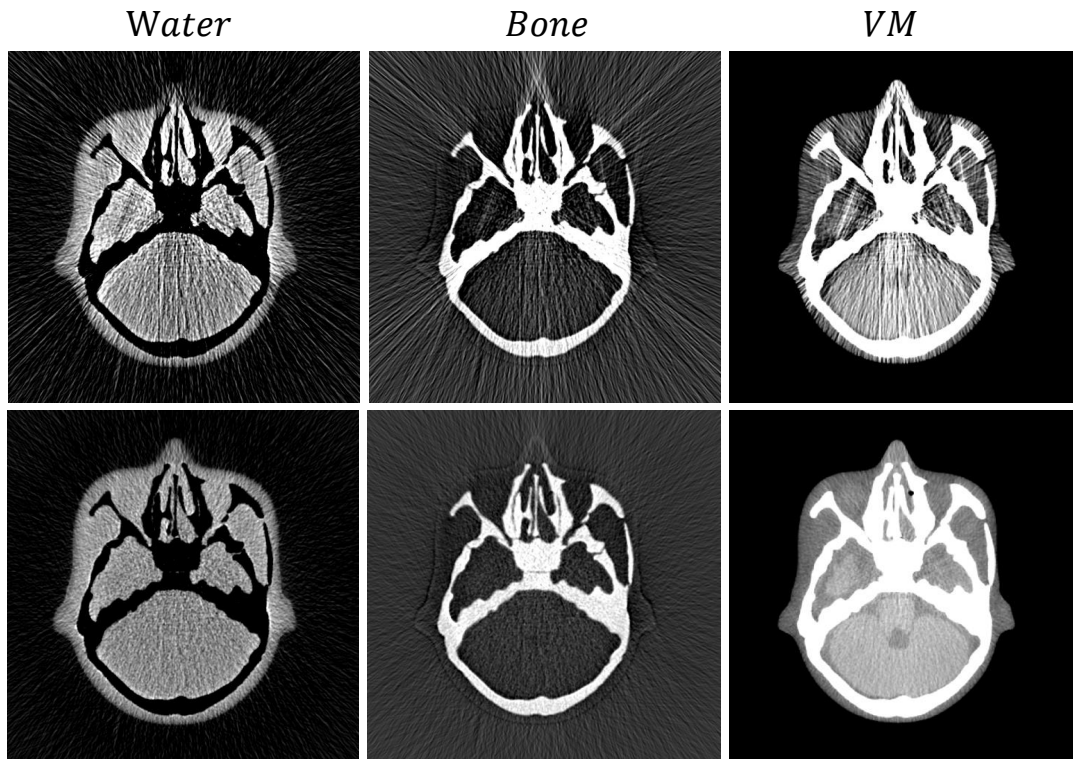


Figure 4. Results of first-pass material decomposition (1st and 3rd rows) and physics model-guided material decomposition (2nd and 4th rows) at two head phantom sections. Display windows for the water, bone and VM images are [-500, 2000] mg/ml, [0, 2000] mg/ml, [-150, 150] HU, respectively.

CBCT system showed its effectiveness of improving image quality in terms of SNR, CNR and low-signal artifact suppression.

Further investigations of our method include more rigorous and broader performance evaluations. Correlated scatter correction for dual-layer FPD is also under development, which will be utilized together with our proposed pMD algorithm here to fully assess the cone-beam CT spectral imaging capability in the near future.

## 5. ACKNOWLEDGEMENTS

This project was supported in part by grants from the National Natural Science Foundation of China (No. U20A20169 and No. 12075130).

## REFERENCES

- [1] Tang, X., Krupinski, E. A., Xie, H. and Stillman, A. E. (2018), On the data acquisition, image reconstruction, cone beam artifacts, and their suppression in axial MDCT and CBCT – A review. *Med. Phys.*, 45: e761-e782.
- [2] Wu, P., Sisniega, A., Stayman, J.W., Zbijewski, W., Foos, D., Wang, X., Khanna, N., Aygun, N., Stevens, R.D. and Siewerdsen, J.H. (2020), Cone-beam CT for imaging of the head/brain: Development and assessment of scanner prototype and reconstruction algorithms. *Med. Phys.*, 47: 2392-2407.
- [3] Wang, W., Ma, Y., Tivnan M, Li J, Gang, G. J., Zbijewski, W., Lu, M., Zhang, J., Star-Lack, J., Colbeth, R.E., Stayman, JW. High-resolution model-based material decomposition in dual-layer flat-panel CBCT. *Med. Phys.* 2021 Jul 17.
- [4] Shi, L., Lu, M., Bennett, N.R., Shapiro, E., Zhang, J., Colbeth, R., Star-Lack, J. and Wang, A.S. (2020), Characterization and potential applications of a dual-layer flat-panel detector. *Med. Phys.*, 47: 3332-3343.

- [5] Gao, H., Cohen, A., Imai, Y. Quantitative Uniformity of Iodinated Contrast Across the Z-Coverage of Large Cone-Angle CT. in Proceedings of 3rd CT meeting. 2014, pp. 220-223
- [6] Stenner, P., Berkus, T. and Kachelriess, M. (2007), Empirical dual energy calibration (EDEC) for cone-beam computed tomography. Med. Phys., 34: 3630-3641.